
Understanding the impact of data distribution on Q -learning with function approximation

Pedro P. Santos^{1,2}

Francisco S. Melo^{1,2}

Alberto Sardinha^{1,2}

Diogo S. Carvalho^{1,2}

¹INESC-ID.

²Instituto Superior Técnico, University of Lisbon.

Abstract

In this work, we study the interplay between the data distribution and Q -learning-based algorithms with function approximation. We provide a unified theoretical and empirical analysis as to why different properties of the data distribution can contribute to regulate sources of algorithmic instability. First, we study theoretical bounds on the performance of approximate dynamic programming algorithms. Second, we provide a novel four-state MDP that highlights the impact of the data distribution in the performance of a Q -learning algorithm with function approximation, both in online and offline settings. Finally, we experimentally assess the impact of the data distribution properties in the performance of offline Q -learning-based algorithms. Our results emphasize the key role played by data distribution properties while regulating algorithmic stability. We provide a systematic and comprehensive study of the topic by connecting different lines of research, as well as validating and extending previous results, both theoretically and empirically.

1 INTRODUCTION

Recent years witnessed significant progress in solving challenging problems across various domains using reinforcement learning (RL) [Mnih et al., 2015, Silver et al., 2017, Lillicrap et al., 2016]. Q -learning algorithms with function approximation are among the most used methods. However, extending of Q -learning convergence guarantees to function approximation settings is hard, especially for the case of large capacity approximators, and several works analyze the unstable behavior of such algorithms both experimentally [van Hasselt et al., 2018, Fu et al., 2019] and theoretically [Zhang et al., 2021, Carvalho et al., 2020].

However, only a few works focus their attention on the study of the interplay between the data distribution, i.e., the distribution used to sample experience or the distribution induced by a dataset of transitions, and the outcome of the learning process [Kumar et al., 2020a, Fu et al., 2019]. Such research direction is the main focus of this work and comprises an important object of study since previous articles identified it as a potential source of instability [Kumar et al., 2020a].

We center our study around the following research question: *which data distributions lead to improved algorithmic stability and performance?* Hence, we investigate how different data distribution properties influence performance in the context of off-policy RL algorithms with function approximation. We primarily focus our attention on offline control RL settings [Levine et al., 2020] with discrete action spaces, in which an RL algorithm aims to learn reward-maximizing behavior using previously collected data without additional interaction with the environment. Nevertheless, our conclusions are also relevant in online RL settings, particularly for algorithms that rely on large-scale replay buffering.

This work contributes to a deeper understanding regarding the influence of the data distribution properties in the performance of approximate dynamic programming (ADP) methods. We provide a systematic and comprehensive study of the topic by connecting different lines of research, as well as validating and extending previous results, both theoretically and empirically. In particular, we first review theoretical bounds on the performance of ADP methods. We provide new interpretations of currently proposed bounds, highlight the close relationship between different properties of the data distribution and the tightness of the bounds, and motivate high entropy distributions from a game-theoretical point of view in the form of a novel theorem. Second, we propose a new four-state MDP that illustrates how the data distribution can impact algorithmic performance both in online and offline RL settings. Finally, we experimentally assess the impact of the data distribution in the performance of offline Q -learning-based algorithms with function approximation under a diverse set of environments.

2 BACKGROUND

In RL [Sutton and Barto, 2018], the agent-environment interaction is modeled as an MDP, formally defined as a tuple $(\mathcal{S}, \mathcal{A}, p, p_0, r, \gamma)$, where \mathcal{S} denotes the state space, \mathcal{A} denotes the action space, $p : \mathcal{S} \times \mathcal{A} \rightarrow \mathcal{P}(\mathcal{S})$ is the state transition probability function with $\mathcal{P}(\mathcal{S})$ being the set of distributions on \mathcal{S} , $p_0 \in \mathcal{P}(\mathcal{S})$ is the initial state distribution, $r : \mathcal{S} \times \mathcal{A} \rightarrow \mathbb{R}$ is the reward function, and $\gamma \in (0, 1)$ is a discount factor. At each step, the agent observes the state of the environment $s_t \in \mathcal{S}$ and chooses an action $a_t \in \mathcal{A}$. Depending on the chosen action, the environment evolves to state $s_{t+1} \in \mathcal{S}$ with probability $p(s_{t+1}|s_t, a_t)$, and the agent receives a reward r_t with expectation given by $r(s_t, a_t)$. A policy, $\pi(a|s) : \mathcal{S} \rightarrow \mathcal{P}(\mathcal{A})$, is a mapping encoding the preferences of the agent. We denote by P^π the $|\mathcal{S}| \times |\mathcal{S}|$ matrix with elements $P^\pi(s_t, s_{t+1}) = \mathbb{E}_{a \sim \pi(a|s_t)} [p(s_{t+1}|s_t, a)]$. A trajectory, $\tau = (s_0, a_0, \dots, s_\infty, a_\infty)$, comprises a sequence of states and actions. The probability of trajectory τ under policy π is given by $\rho_\pi(\tau) = p_0(s_0) \prod_{t=0}^{\infty} \pi(a_t|s_t) p(s_{t+1}|s_t, a_t)$. The discounted reward objective can be written as $J(\pi) = \mathbb{E}_{\tau \sim \rho_\pi} [\sum_{t=0}^{\infty} \gamma^t r(s_t, a_t)]$. The objective of the agent is to find an optimal policy π^* that maximizes the above objective function, i.e., $J(\pi^*) \geq J(\pi), \forall \pi$. RL algorithms usually involve the estimation of the optimal Q -function, Q^* , satisfying the Bellman optimality equation: $Q^*(s_t, a_t) = r(s_t, a_t) + \gamma \mathbb{E}_{s_{t+1} \sim p} [\max_{a_{t+1} \in \mathcal{A}} Q^*(s_{t+1}, a_{t+1})]$.

Q -learning [Watkins and Dayan, 1992] allows an agent to learn directly from raw experience in an online, incremental fashion, by estimating optimal Q -values from observed trajectories using the temporal difference (TD) update rule: $Q(s_t, a_t) \leftarrow Q(s_t, a_t) + \alpha [r_t + \gamma \max_{a_{t+1} \in \mathcal{A}} Q(s_{t+1}, a_{t+1}) - Q(s_t, a_t)]$. Convergence to the optimal policy is guaranteed if all state-action pairs are visited infinitely often and the learning rate α is appropriately decayed. Usually, in order to adequately explore the $\mathcal{S} \times \mathcal{A}$ space, an ϵ -greedy policy is used. An ϵ -greedy policy chooses, most of the time, an action that has maximal Q -value for the current state, but with probability ϵ selects a random action instead.

In ADP, Q -values are approximated by a differentiable function Q_ϕ , where ϕ denotes the learnable parameters of the model. ADP algorithms, such as the well-known deep Q -network (DQN) algorithm [Mnih et al., 2015], usually interleave two phases: (i) a sampling phase, where parameters ϕ are kept fixed and a behavior policy (e.g., ϵ -greedy policy) is used to collect transitions (s_t, a_t, r_t, s_{t+1}) and store them into a replay buffer (denoted by \mathcal{B}); and (ii) an update phase, where transitions are sampled from \mathcal{B} and used to update parameters ϕ such that $\mathcal{L}_\phi = \mathbb{E}_{\mathcal{B}} [(r_t + \gamma \max_{a_{t+1} \in \mathcal{A}} Q_{\phi^-}(s_{t+1}, a_{t+1}) - Q_\phi(s_t, a_t))^2]$, is minimized, where ϕ^- denotes the parameters of the target network Q_{ϕ^-} , a periodic copy of the behavior network. The

pseudocode of a generic Q -learning algorithm with function approximation can be found in Appendix A.

Offline RL [Levine et al., 2020] aims at finding an optimal policy with respect to $J(\pi)$ using a static dataset of experience. The fundamental problem of offline RL is distributional shift: out-of-distribution samples lead to algorithmic instabilities and performance loss, both at training and deployment time. The conservative Q -learning (CQL) [Kumar et al., 2020b] algorithm is an offline RL algorithm that aims to estimate the optimal Q -function using ADP techniques, while mitigating the impact of distributional shift. Precisely, the algorithm avoids the overestimation of out-of-distribution actions by considering an additional conservative penalty term of the type $\mathcal{L}_c = \mathbb{E}_{s \sim \mathcal{B}, a \sim \nu} [Q_\phi(s, a)]$, yielding the global objective $\mathcal{L}_{\text{CQL}} = \mathcal{L}_\phi + k \mathcal{L}_c, k \in \mathbb{R}_0^+$, which the algorithm aims to minimize. Distribution $\nu(a|s)$ is chosen adversarially such that it selects overestimated Q -values with high probability, e.g., by maximizing \mathcal{L}_c .

3 RELATED WORK

There are different lines of research closely related to our work. We start by referring early studies that analyze the unstable behavior of off-policy learning algorithms and the harmful learning dynamics that can lead to the divergence of the function parameters [Kolter, 2011, Tsitsiklis and van Roy, 1996, Tsitsiklis and Van Roy, 1997, Baird, 1995]. Different works provide examples that highlight the unstable behavior of ADP methods [Baird, 1995, Tsitsiklis and van Roy, 1996, Kolter, 2011]. Kolter [2011] provides an example that highlights the dependence of the off-policy distribution on the approximation error of the algorithm. In Sec. 4.2, we propose a novel four-state MDP that highlights the impact of the data distribution in the performance of ADP methods. We further explore how off-policy algorithms can be affected by data distribution changes, under diverse settings. Unlike previous works, we consider both offline settings comprising static data distributions, and online settings in which data distributions are induced by replay buffers.

Another line of research related to our study involves works that analyze error propagation in ADP methods, deriving error bounds on the performance of approximate policy iteration [Kakade and Langford, 2002, Munos, 2003] and approximate value iteration [Munos, 2005, Munos and Szepesvári, 2008] algorithms. Munos [2003] provides error bounds for approximate policy iteration using quadratic norms, as well as bounds on the error between the performance of the policies induced by the value iteration algorithm and the optimal policy as a function of weighted L_p -norms of the approximation errors [Munos, 2005]. Munos and Szepesvári [2008] develop a theoretical analysis of the performance of sampling-based fitted value iteration, providing finite-time bounds on the performance of the algorithm. Yang et al. [2019] establish algorithmic and statistical rates of conver-

gence for the iterative sequence of Q -functions obtained by the DQN algorithm. Chen and Jiang [2019] further improve the bounds of the previous studies, while considering an offline RL setting. Common to all these works is the dependence of the derived bound on a data distribution-related concentrability coefficient. In this work, we review concentrability coefficients in Sec. 4.1, providing new insights and a novel motivation for the use of high entropy data distributions through the lens of robust optimization. We also connect our experimental results, presented in Sec. 5, with theoretical results from the aforementioned articles.

Our study is also related with recent works that investigate the stability of deep RL methods [van Hasselt et al., 2018, Fu et al., 2019, Kumar et al., 2019, 2020a, Liu et al., 2018, Zhang et al., 2021], as well as the development of RL methods specifically suited for offline settings [Agarwal et al., 2019, Mandelkar et al., 2021, Levine et al., 2020]. Kumar et al. [2020a] identify that Q -learning-related methods can exhibit pathological interactions between the data distribution and the policy being learnt, leading to potential instability. Fu et al. [2019] investigate how different components of DQN play a role in the emergence of the deadly triad. In particular, the authors assess the performance of DQN with different sampling distributions, finding that higher entropy distributions tend to perform better. Agarwal et al. [2019] provide a set of ablation studies that highlight the impact of the dataset size and diversity in offline learning settings. In this work, we provide a study of the impact of different data distribution properties in the performance of offline RL algorithms in Sec. 5. We validate and extend previous results, as well as connect our experimental findings with theoretical results. As opposed to previous works, we provide a systematic study of the topic with thorough attention to detail, featuring experimental setups explicitly designed to rigorously study the impact of the data distribution in the stability of the offline learning algorithms.

Also related to our work, offline RL datasets have been recently proposed [Fu et al., 2020, Gülçehre et al., 2020, Qin et al., 2021] in an attempt to benchmark progress in offline RL. Such datasets, which are usually collected by running an exploratory policy on the environment or by storing the contents of the replay buffer at a given point during training, usually differ in properties such as the data diversity and size. In this work, we chose not to use such datasets in order to have complete control over the dataset generation procedure, which allows us to rigorously control different metrics of the datasets and systematically compare our experimental results. Nevertheless, our results are representative of a diverse set of discrete action-space control tasks.

Finally, and concurrently to our work, Schweighofer et al. [2021] study the impact of dataset characteristics on offline RL. Precisely, the authors study the influence of the average dataset return and state-action coverage on the performance of different RL algorithms while controlling the dataset

generation procedure. Despite some similarity with some of the experiments in Sec. 5, we present a much broader picture regarding the impact of the data distribution in the stability of general off-policy RL algorithms, from both theoretical and experimental point-of-views. Additionally, the experimental methodology carried out by both works differs in several aspects, such as the calculation of the dataset metrics used for the presentation of the experimental results or the types of environments used.

4 THE DATA DISTRIBUTION MATTERS

In this section, we investigate how the data distribution can impact the performance of Q -learning-based algorithms with function approximation, theoretically and empirically. We consider both online and offline learning settings.

4.1 THEORETICAL BOUNDS

As discussed in the previous section, different studies analyze error propagation in ADP [Munos, 2003, 2005, Munos and Szepesvári, 2008, Yang et al., 2019, Chen and Jiang, 2019]. Importantly, the tightness of the error upper bounds derived by the aforementioned works depends on different sources of error, one of which consists of a concentrability coefficient C that is dependent on the properties of the data/sampling distribution. The lower the concentrability coefficient C , the tighter the bound.

Munos [2003] introduces the first version of this data-dependent concentrability coefficient, C_1 , which corresponds to a bound on the density of the transition probability function. Specifically, $C_1 = \sup_{s \in \mathcal{S}, a \in \mathcal{A}} \|p(\cdot | s, a) / \mu\|_\infty$, where $\mu \in \mathcal{P}(\mathcal{S})^1$ denotes the sampling distribution. Munos [2005] introduces a different concentrability coefficient, C_2 , related to the discounted average concentrability of future-states on the MDP. Specifically,

$$C_2 = (1 - \gamma)^2 \sum_{m=1}^{\infty} m \gamma^{m-1} c(m), \quad (1)$$

$$c(m) = \sup_{\pi_1, \dots, \pi_m} \left\| \frac{\rho P^{\pi_1} P^{\pi_2} \dots P^{\pi_m}}{\mu} \right\|_\infty, \quad (2)$$

$\mu, \rho \in \mathcal{P}(\mathcal{S})$, and ρ reflects the importance of various regions of the state space and is selected by the practitioner. Munos [2005] and Munos and Szepesvári [2008] note that the assumption introduced by C_1 is stronger than the assumption introduced by (1), which expresses some smoothness property of the future state distribution with respect to μ for an initial distribution ρ .

Farahmand et al. [2010] and Yang et al. [2019] further improve the aforementioned error bounds, replacing the

¹The discussion generalizes for $\mu \in \mathcal{P}(\mathcal{S} \times \mathcal{A})$.

supremum-norm in (2) with a weighted norm

$$c(m) = \sup_{\pi_1, \dots, \pi_m} \left\| \frac{\rho P^{\pi_1} P^{\pi_2} \dots P^{\pi_m}}{\mu} \right\|_{2, \mu}. \quad (3)$$

We let C_3 denote the coefficient defined by (1) and (3). Other works [Antos et al., 2008, Lazaric et al., 2012, 2016, Xie and Jiang, 2020] use concentrability coefficients similar to those defined above to derive upper bounds on the performance of various algorithms.

Unfortunately, although the concentrability coefficients above attempt to provide a closed way to quantify distributional shift, they have limited interpretability. Specifically, it is hard to infer from the aforementioned coefficients which exact sampling distributions should be used. For example, if we consider coefficients C_2 and C_3 , even if we know which parts of the state space are relevant (according to the distribution ρ in (2) and (3)), the computation of the coefficient in (1) still depends on the complex interactions between ρ and the dynamics of the MDP under any possible policy. What can be concluded is that the concentrability coefficient will depend on all states that can be reached by any policy when the starting state distribution is given by ρ . However, it is not obvious which exact target distribution we should aim at when selecting the sampling distribution μ , especially when we do not know the underlying MDP or which regions of the state space are of interest. In the face of such uncertainty, previous works suggest that high coverage of the state space is desirable, assuming upper-bounded concentrability coefficients [Munos and Szepesvári, 2008, Farahmand et al., 2010, Chen and Jiang, 2019, Yang et al., 2019].

More recently, different works study the impact of the data distribution on offline policy evaluation with linear function approximation [Duan and Wang, 2020, Wang et al., 2020]. Wang et al. [2020] show that good data coverage is not sufficient to sample-efficiently perform offline policy evaluation and that significantly stronger assumptions on distributional shift may be needed.

In the next sections, we provide a new interpretation of C_3 as an f -divergence and give a new motivation for the use of maximum entropy sampling distributions.

4.1.1 Concentrability Coefficient as an f -divergence

Letting $\beta = \rho P^{\pi_1} P^{\pi_2} \dots P^{\pi_m}$, we can rewrite (3) as

$$\begin{aligned} \left\| \frac{\beta}{\mu} \right\|_{2, \mu} &= \left(\mathbb{E}_{(s,a) \sim \mu} \left[\left(\frac{\beta(s,a)}{\mu(s,a)} \right)^2 \right] \right)^{1/2} \\ &= \sqrt{\mathcal{D}_f(\beta \parallel \mu) + 1} = \sqrt{\chi^2(\beta \parallel \mu) + 1}, \end{aligned}$$

for $f(x) = x^2 - 1$, where \mathcal{D}_f denotes the f -divergence and χ^2 the chi-square divergence.

4.1.2 Motivating Maximum Entropy Distributions

We start our analysis by noting that optimizing (3) over the distribution μ is hard due to the fact that, as previously noted, we actually want to minimize $\mathcal{D}_f(\beta \parallel \mu)$ with respect to a large set of different β distributions (due to the supremum in (3), as well as the summation in (1)). Furthermore, we usually do not have access to the transition probability function. Therefore, we analyze the problem of picking an optimal μ distribution as a robust optimization problem. Specifically, we formulate a minimax objective where the minimizing player aims at choosing μ to minimize $\mathcal{D}_f(\beta \parallel \mu)$ and the maximizing player chooses β to maximize $\mathcal{D}_f(\beta \parallel \mu)$. We get the following result (proof in Appendix B).

Theorem 4.1. *Let $\mathcal{P}(\mathcal{S} \times \mathcal{A})$ represent the set of probability distributions over $\mathcal{S} \times \mathcal{A}$. Let also $L_\mu : \mathcal{P}(\mathcal{S} \times \mathcal{A}) \rightarrow \mathbb{R}_0^+$ such that $L_\mu(\beta) = \left\| \frac{\beta}{\mu} \right\|_{2, \mu}^2$. The solution μ to*

$$\operatorname{argmin}_{\mu \in \mathcal{P}(\mathcal{S} \times \mathcal{A})} \max_{\beta \in \mathcal{P}(\mathcal{S} \times \mathcal{A})} L_\mu(\beta) \quad (4)$$

is the maximum entropy distribution over $\mathcal{S} \times \mathcal{A}$.

As stated in Theorem 4.1, the maximum entropy distribution, equivalent to the uniform distribution, is the solution to the robust optimization problem. This result provides a theoretical justification for the benefits of using high entropy sampling distributions, as suggested by previous works [Kakade and Langford, 2002, Munos, 2003]: uniform distributions ensure coverage over the state-action space, contributing to keep concentrability coefficients low.

4.2 FOUR-STATE MDP

In this section, we study how the data distribution can influence the performance of a Q -learning algorithm with function approximation, under a four-state MDP (Fig. 1). We show that the data distribution can significantly influence the quality of the resulting policies and affect the stability of the learning algorithm. Due to space constraints, we focus our discussion on the main conclusions and refer to Appendix B for an in-depth discussion, including additional experiments and insights. This section shows that the data distribution can play an active role regulating algorithmic stability.

We focus our attention to non-terminal states s_1 and s_2 . In state s_1 the correct action is a_1 , whereas in state s_2 the correct action is a_2 . We set $\gamma = 1$. We consider a linear function approximator $Q_w(s_t, a_t) = w^\top \phi(s_t, a_t)$, where ϕ is a feature mapping, defined as $\phi(s_1, a_1) = [1, 0, 0]^\top$, $\phi(s_1, a_2) = [0, 1, 0]^\top$, $\phi(s_2, a_1) = [\alpha, 0, 0]^\top$, and $\phi(s_2, a_2) = [0, 0, 1]^\top$, with $\alpha \in [1, 3/2)$. As can be seen, the capacity of the function approximator is limited and there exists a correlation between $Q_w(s_1, a_1)$ and $Q_w(s_2, a_1)$. This will be key to the results that follow.

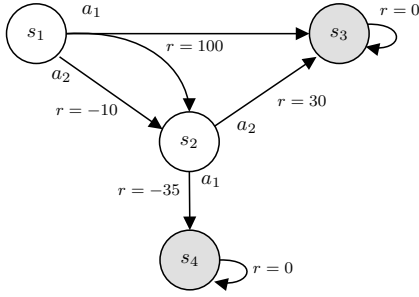


Figure 1: Four-state MDP, with states $\{s_1, s_2, s_3, s_4\}$ and actions $\{a_1, a_2\}$. State s_1 is the initial state and states s_3 and s_4 are terminal (absorbing) states. All actions are deterministic except for the state-action pair (s_1, a_1) , where $p(s_3|s_1, a_1) = 0.99$ and $p(s_2|s_1, a_1) = 0.01$. The reward function is $r(s_1, a_1) = 100$, $r(s_1, a_2) = -10$, $r(s_2, a_1) = -35$ and $r(s_2, a_2) = 30$.

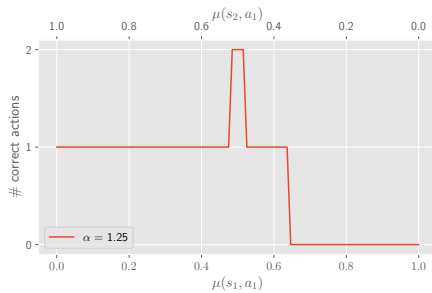
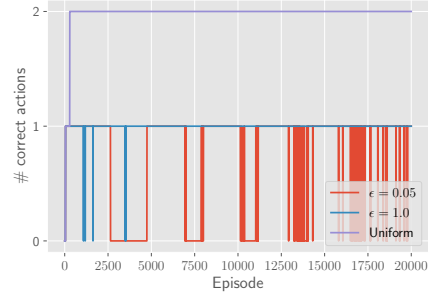


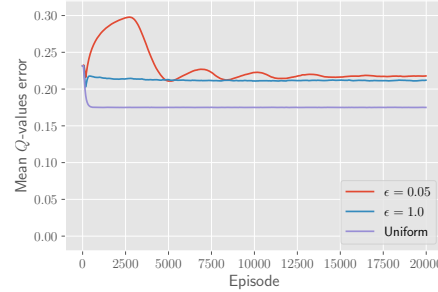
Figure 2: The number of correct actions at states s_1 and s_2 for different data distributions ($\alpha = 1.25$).

4.2.1 Offline Learning

We consider an offline RL setting and denote by μ the distribution over the $\mathcal{S} \times \mathcal{A}$ space induced by a static dataset of transitions. We focus our attention on probabilities $\mu(s_1, a_1)$ and $\mu(s_2, a_1)$, since these are the probabilities associated with the two partially correlated state-action pairs. Fig. 2 displays the influence of the data distribution, namely the proportion between $\mu(s_1, a_1)$ and $\mu(s_2, a_1)$, on the number of correct actions yielded by the learned policy. We identify three regimes: (i) when $\mu(s_1, a_1) \approx 0.5$, we learn the optimal policy; (ii) if $\mu(s_1, a_1) < (\approx 0.48)$ or $(\approx 0.52) < \mu(s_1, a_1) < (\approx 0.65)$, the policy is only correct at one of the states; (iii) if $\mu(s_1, a_1) > (\approx 0.65)$, the policy is wrong at both states. The results above show that, due to the limited power and correlation between features, the data distribution impacts performance as the number of correct actions is directly dependent on the properties of the data distribution. As our results show, due to bootstrapping, it is possible that under certain data distributions neither action is correct.



(a) Number of correct actions.



(b) Q -values mean error.

Figure 3: Experiments for different exploratory policies with an infinitely-sized replay buffer.

4.2.2 Online Learning with Unlimited Replay

Instead of considering a fixed μ distribution, we now consider a setting where μ is dynamically induced by a replay buffer obtained using ϵ -greedy exploration. Figure 3 shows the results when $\alpha = 1.2$, under: (i) an ϵ -greedy policy with $\epsilon = 1.0$; and (ii) an ϵ -greedy policy with $\epsilon = 0.05$. We consider a replay buffer with unlimited capacity. We use a uniform synthetic data distribution as baseline. As seen in Fig. 3, the baseline outperforms all other data distributions, as expected. Regarding the ϵ -greedy policy with $\epsilon = 1.0$, the agent is only able to pick the correct action at state s_1 , featuring a higher average Q -value error in comparison to the baseline. This is due to the fact that the stationary distribution of the MDP under the fully exploratory policy is too far from the uniform distribution to retrieve the optimal policy. Finally, for the ϵ -greedy policy with $\epsilon = 0.05$, the performance of the agent further deteriorates. Such exploratory policy induces oscillations in the Q -values (Fig. 3 (b)), which eventually damp out as learning progresses. The oscillations are due to an undesirable interplay between the features and the data distribution: exploitation may cause abrupt changes in the data distribution and hinder learning.

4.2.3 Online Learning with Limited Replay Capacity

Finally, we consider an experimental setting where the replay buffer has limited capacity and study the impact of its

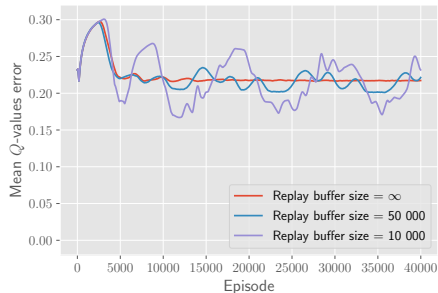


Figure 4: Q -values error under the ($\epsilon = 0.05$)-greedy policy for different replay capacities.

size in the stability of the algorithm. Figure 4 displays the results obtained with the ϵ -greedy policy with $\epsilon = 0.05$, while varying the capacity of the replay buffer. As can be seen, as the replay buffer size increases the oscillations in the Q -values errors are smaller. The undesirable interplay previously observed under the infinitely-sized replay buffer repeats. However, the smaller the replay buffer capacity, the more the data distribution induced by the contents of the replay buffer is affected by changes to the current exploratory policy, i.e., exploitation leads to more abrupt changes in the data distribution, which, in turn, drive abrupt changes to the Q -values. For the infinitely-sized replay buffer the amplitude of the oscillations is dampened because previously stored experience contributes to make the data distribution more stationary, not as easily achieved by smaller buffers.

4.2.4 Discussion

We presented a set of experiments using a four-state MDP that show how the data distribution can influence the performance of the resulting policies and the stability of the learning algorithm. First, we showed that, under an offline RL setting, the retrieved number of correct actions is directly dependent on the properties of the data distribution due to an undesirable correlation between features. Second, not only the quality of the retrieved policies depends on the data collection mechanism, but also an undesirable interplay between the data distribution and the function approximator can arise: exploitation can lead to abrupt changes in the data distribution and hinder learning. Finally, we showed that the replay buffer size can also affect the learning dynamics.

5 EMPIRICALLY ASSESSING THE IMPACT OF THE DATA DISTRIBUTION IN OFFLINE RL

In the present section, we experimentally assess the impact of different data distribution properties on the performance of the offline DQN and CQL algorithms. We evaluate the performance of the RL algorithms under six different en-

vironments: the *grid 1* and *grid 2* environments consist of standard tabular environments with highly uncorrelated state features, the *multi-path* environment is a hard exploration environment, and the *pendulum*, *mountaincar* and *cartpole* environments are benchmarking environments featuring a continuous state-space domain. All reported values are calculated by aggregating the results of different training runs. The description of the experimental environments and the experimental methodology, as well as the complete results can be found in Appendix C. The developed software can be found [here](#). We also provide an interactive dashboard with all our experimental results at <https://rl-data-distribution.herokuapp.com/>.

In this section, we denote by μ the data distribution over state-action pairs induced by a static dataset of transitions. We consider two types of offline datasets: (i) *ϵ -greedy* datasets, generated by running an ϵ -optimal policy on the MDP, i.e., a policy that is ϵ -greedy with respect to the optimal Q -values with $\epsilon \in [0, 1]$; and (ii) *Boltzmann(t)* datasets, generated by running a Boltzmann policy with respect to the optimal Q -values with temperature coefficient $t \in [-10, 10]$. Additionally, we artificially force, for some of the generated datasets, that they have full coverage over the $\mathcal{S} \times \mathcal{A}$ space. We do this by running an additional procedure that enforces that each state-action pair appears at least once in the dataset.

Two aspects are worth mentioning. First, in all environments, the sampling error is low due to the highly deterministic nature of the underlying MDPs. Thus, a single next-state sample is sufficient to correctly evaluate the Bellman optimality operator. Second, the function approximator has enough capacity to correctly represent the optimal Q -function, a property known as *realizability* [Chen and Jiang, 2019].

5.1 HIGH ENTROPY IS BENEFICIAL

We start our analysis by studying the impact of the dataset distribution entropy, $\mathcal{H}(\mu)$, on the performance of the offline RL algorithms. Figure 5 displays the obtained experimental results. As can be seen, under all environments and for both offline algorithms, high entropy distributions tend to achieve increased rewards. In other words, distributions with an entropy close to that of the uniform distribution appear to be well suited to be used in offline learning settings. Such observation is inline with the discussion drawn in Sec. 4.1: high entropy distributions contribute to keep concentrability coefficients low and, thus, mitigate algorithmic instabilities.

Importantly, we do not claim that high entropy distributions are the only distributions suitable to be used. As can be seen in Fig. 5, certain lower-entropy distributions also perform well. In the next sections, we investigate which other properties of the distribution are of benefit to offline RL.

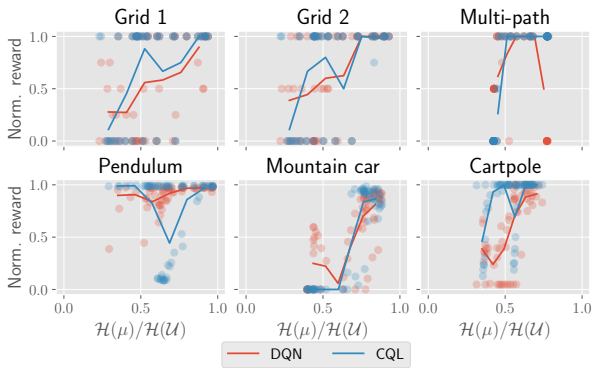


Figure 5: Average normalized rollouts reward for datasets with different normalized entropies.

5.2 DATASET COVERAGE MATTERS

We now study the impact of the dataset coverage, i.e., the diversity of the transitions in the dataset, in the performance of the offline agents. In order to keep the discussion concise, in this section we focus our attention on ϵ -greedy datasets, and refer to Appendix C for the complete results.

We start by focusing our attention on the offline DQN algorithm. Figure 6 (a) displays the obtained experimental results. As can be seen, DQN struggles to achieve optimal rewards for low ϵ values, i.e., even though the algorithm is provided with optimal or near-optimal trajectories, it is unable to steadily learn under such setting. However, as ϵ increases the performance of the algorithm increases, eventually decaying again for high ϵ values. Such results suggest that a certain degree of data coverage is required by DQN to robustly learn in an offline manner, despite being provided with high quality data (rich in rewards). On the other hand, the decay in performance for highly exploratory policies under some environments can be explained by the fact that such policies induce trajectories that are poor in reward (this is further explored in the next section). Figure 6 (b) displays the obtained experimental results under the exact same datasets, except that we enforce coverage over the $\mathcal{S} \times \mathcal{A}$ space. We note a substantial improvement in the performance of DQN across all environments, supporting our hypothesis that data coverage plays an important role regulating the stability of offline RL algorithms.

The CQL algorithm appears to perform more robustly than DQN. Particularly, as seen in Fig. 6 (a), CQL is able to robustly learn with low ϵ values, i.e., using optimal or near optimal trajectories that feature low coverage. Additionally, no substantial performance gain is observed under the offline CQL agent by enforcing dataset coverage (Fig. 6 (b)).

The finding that data coverage appears to play an important role regulating the performance of DQN, even when considering high quality, near optimal trajectories, is in-

line with the discussion presented in Sec. 4.1. One could argue that we are only interested in correctly estimating the Q -values along an optimal trajectory, however, due to the bootstrapped nature of the updates, error in the estimation of the Q -values for adjacent states can erroneously affect the estimation of the Q -values along the optimal trajectory. This reasoning is suggested by concentrability coefficients. If we consider distribution ρ from (2) or (3) to be the uniform distribution over the states of the optimal trajectory and zero otherwise, we can see that the concentrability coefficient given by (1) still depends on other states than those of the optimal trajectory. Precisely, the coefficient depends on all the states that can be reached by any policy when the starting state is sampled according to ρ (the importance of each state geometrically decays depending on their distance to the optimal trajectory). Therefore, in order to keep the concentrability coefficient low it is important that such states are present in the dataset. On the other hand, CQL is still able to robustly learn using high quality trajectories independently of the data coverage because of its pessimistic nature. Since the algorithm penalizes the Q -values for actions that are underrepresented in the dataset, the error for adjacent states is not propagated in the execution of the algorithm.

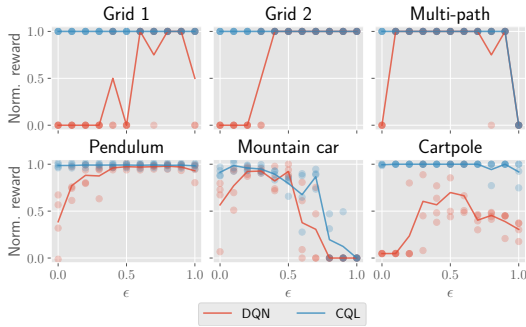
In this section, we considered datasets that are, in general, aligned and close to that induced by optimal policies. What happens if our data is collected by arbitrary policies? Offline learning under such settings can be harder. We investigate the impact of the trajectory quality in the next section.

5.3 CLOSENESS TO OPTIMAL POLICY MATTERS

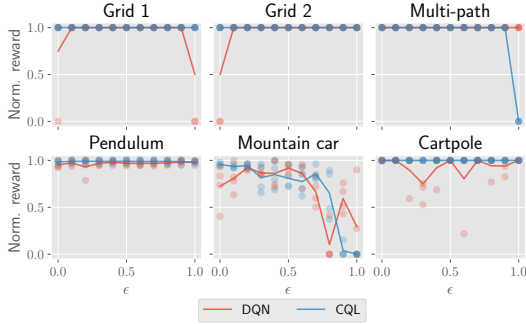
Now, we investigate how offline agents can be affected by the quality of the trajectories contained in the dataset. More precisely, we study how the statistical distance between distribution μ and the distribution induced by one of the optimal policies of the MDP, d_{π^*} , affects offline learning.

The obtained experimental results are portrayed in Fig. 7. We consider a wide spectrum of behavior policies, from optimal to anti-optimal policies, as well as from fully exploitative to fully exploratory policies. As can be seen, as the statistical distance between distribution μ and the closest distribution induced by one of the optimal policies increases, the lower the rewards obtained, irrespectively of the algorithm. We can also observe an increase in obtained rewards when dataset coverage is enforced (Fig. 7 (b)) in comparison to when dataset coverage is not enforced (Fig. 7 (a)).

At first sight, our results appear intuitive if we focus on Fig. 7 (a), where dataset coverage is not enforced: if the policy used to collect the dataset is not good enough, it will fail to collect trajectories rich in rewards, key to learn reward-maximizing behavior. As an example, if the policy used to collect the data is highly exploratory, the agent will likely



(a) Dataset coverage not enforced.



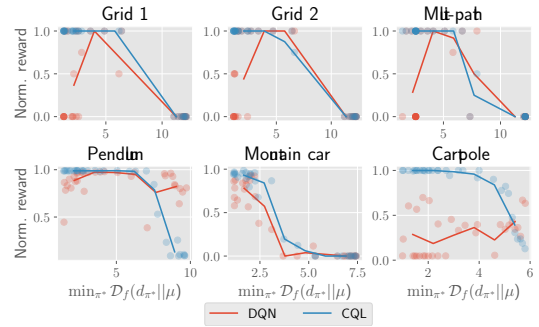
(b) Dataset coverage enforced.

Figure 6: Average normalized rollouts reward under ϵ -greedy datasets for different ϵ values.

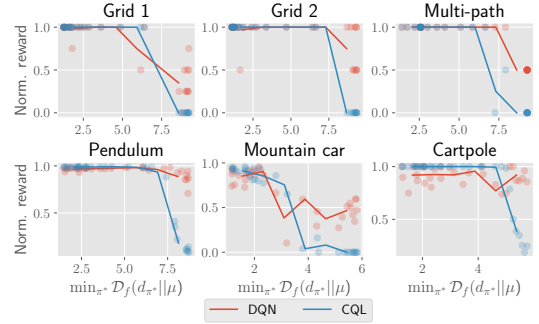
not reach high rewarding states and the learning signal may be too weak to learn an optimal policy in an offline manner.

However, the results displayed in Fig. 7 (b), i.e., the experimental setting in which dataset coverage is enforced, reveal a rather less intuitive finding: despite the fact that all datasets feature full coverage over the $S \times \mathcal{A}$ space, if the statistical distance between the two distributions is high, we observe a deterioration in algorithmic performance. In other words, despite the fact that the datasets contain all the information that can be retrieved from the environment (including transitions rich in reward), offline learning can still be hard if the behavior policy is too distant from the optimal policy. Such observation can possibly be explained by the fact that distributions far from the optimal policy prevent the propagation of information, namely Q -values, during the execution of the offline RL algorithm.

Given the experimental results presented in this section, we hypothesize that it is important for the data distribution to be aligned with that of optimal policies, not only to ensure that trajectories are rich in reward, but also to mitigate algorithmic instabilities. Our experimental results suggest that the assumption of a bounded concentrability coefficient, as discussed in Sec. 4.1, may not be enough to robustly learn in an offline manner and that more stringent assumptions on the data distribution are required. Wang et al. [2020] reach



(a) Dataset coverage not enforced.



(b) Dataset coverage enforced.

Figure 7: Average normalized rollouts reward; the x-axis encodes the statistical distance between μ and the closest distribution induced by one of the optimal policies, d_{π^*} .

a similar conclusion, from a theoretical perspective.

5.4 DISCUSSION

This section experimentally assessed the impact of different data distribution properties in the performance of offline Q -learning algorithms with function approximation, showing that the data distribution greatly impacts algorithmic performance. Our results suggest that: (i) high entropy data distributions are well-suited for learning in an offline manner; and (ii) a certain degree of data diversity (data coverage) and data quality (closeness to distributions induced by optimal policies) are jointly desirable for robust offline learning.

Finally, as seen in Fig. 7, the performance of DQN and CQL is dependent on the exact experimental setting, namely on whether coverage is enforced or not. When dataset coverage is not enforced (Fig. 7 (a)), CQL outperforms DQN, especially for distributions close to that of optimal policies (as can also be seen in Fig. 6 (a)). However, when coverage is enforced (Fig. 7 (b)), DQN outperforms CQL, especially for distributions that are more distant to that of optimal policies, as can be seen in Fig. 7 (b). This is due to the fact that both algorithms balance the tradeoff between optimism and pessimism in different ways. DQN is very optimistic and fails under low-coverage settings, since it propagates erroneous

Q -values during the execution of the algorithm. However, due to its optimistic nature, it outperforms CQL when coverage is enforced, taking advantage of information that is underrepresented in the dataset. CQL, on the other hand, outperforms DQN under low coverage settings since, due to its pessimistic nature, prevents the propagation of erroneous Q -values. However, when valuable but underrepresented information is present in the dataset, the pessimism of CQL prevents learning, and CQL is outperformed by DQN.

6 CONCLUSION

In this work, we investigate the interplay between the data distribution and Q -learning-based algorithms with function approximation. We analyze how different properties of the data distribution affect performance in both online and offline RL settings. We show, both theoretically and empirically, that: (i) high entropy data distributions contribute to mitigate sources of algorithmic instability; and (ii) different properties of the data distribution influence the performance of RL methods with function approximation. We provide a thorough experimental assessment of the performance of both DQN and CQL algorithms under several types of offline datasets, connecting our experimental results with theoretical findings of previous works.

The experimental results presented herein provide useful insights for the development of improved data processing techniques for offline RL, which should be valuable for future research. For example, our results suggest that maximum entropy exploration methods [Hazan et al., 2018] can be well suited for the construction of datasets for offline RL, naïve dataset concatenation can lead to deterioration in performance, and that, by simply reweighting or discarding of training data, it is possible to substantially improve performance of offline RL algorithms.

References

Martin Abadi, Ashish Agarwal, Paul Barham, Eugene Brevdo, Zhifeng Chen, Craig Citro, Greg S. Corrado, Andy Davis, Jeffrey Dean, Matthieu Devin, Sanjay Ghemawat, Ian Goodfellow, Andrew Harp, Geoffrey Irving, Michael Isard, Yangqing Jia, Rafal Jozefowicz, Lukasz Kaiser, Manjunath Kudlur, Josh Levenberg, Dandelion Mané, Rajat Monga, Sherry Moore, Derek Murray, Chris Olah, Mike Schuster, Jonathon Shlens, Benoit Steiner, Ilya Sutskever, Kunal Talwar, Paul Tucker, Vincent Vanhoucke, Vijay Vasudevan, Fernanda Viégas, Oriol Vinyals, Pete Warden, Martin Wattenberg, Martin Wicke, Yuan Yu, and Xiaoqiang Zheng. TensorFlow: Large-scale machine learning on heterogeneous systems, 2015.

Rishabh Agarwal, Dale Schuurmans, and Mohammad

Norouzi. An optimistic perspective on offline reinforcement learning. *CoRR*, abs/1907.04543, 2019.

Andras Antos, Csaba Szepesvari, and Rémi Munos. Learning near-optimal policies with Bellman-residual minimization based fitted policy iteration and a single sample path. *Machine Learning*, 71:89–129, 2008.

Leemon Baird. Residual algorithms: Reinforcement learning with function approximation. In *In Proceedings of the Twelfth International Conference on Machine Learning*, pages 30–37. Morgan Kaufmann, 1995.

Diogo Carvalho, Francisco S Melo, and Pedro Santos. A new convergent variant of q-learning with linear function approximation. *Advances in Neural Information Processing Systems*, 33:19412–19421, 2020.

Jinglin Chen and Nan Jiang. Information-theoretic considerations in batch reinforcement learning. *CoRR*, abs/1905.00360, 2019.

Yaqi Duan and Mengdi Wang. Minimax-optimal off-policy evaluation with linear function approximation. *CoRR*, abs/2002.09516, 2020.

Amir-massoud Farahmand, Csaba Szepesvári, and Rémi Munos. Error propagation for approximate policy and value iteration. In J. Lafferty, C. Williams, J. Shawe-Taylor, R. Zemel, and A. Culotta, editors, *Advances in Neural Information Processing Systems*, volume 23, 2010.

Justin Fu, Aviral Kumar, Matthew Soh, and Sergey Levine. Diagnosing bottlenecks in deep q-learning algorithms. *CoRR*, abs/1902.10250, 2019.

Justin Fu, Aviral Kumar, Ofir Nachum, George Tucker, and Sergey Levine. D4RL: datasets for deep data-driven reinforcement learning. *CoRR*, abs/2004.07219, 2020.

Çağlar Gülçehre, Ziyu Wang, Alexander Novikov, Tom Le Paine, Sergio Gómez Colmenarejo, Konrad Zolna, Rishabh Agarwal, Josh Merel, Daniel J. Mankowitz, Cosmin Paduraru, Gabriel Dulac-Arnold, Jerry Li, Mohammad Norouzi, Matt Hoffman, Ofir Nachum, George Tucker, Nicolas Heess, and Nando de Freitas. RL unplugged: Benchmarks for offline reinforcement learning. *CoRR*, abs/2006.13888, 2020.

Elad Hazan, Sham M. Kakade, Karan Singh, and Abby Van Soest. Provably efficient maximum entropy exploration. *CoRR*, abs/1812.02690, 2018.

Matt Hoffman, Bobak Shahriari, John Aslanides, Gabriel Barth-Maron, Feryal Behbahani, Tamara Norman, Abbas Abdolmaleki, Albin Cassirer, Fan Yang, Kate Baumli, Sarah Henderson, Alex Novikov, Sergio Gomez Colmenarejo, Serkan Cabi, Çağlar Gulcehre, Tom Le Paine,

- Andrew Cowie, Ziyu Wang, Bilal Piot, and Nando de Freitas. Acme: A research framework for distributed reinforcement learning, 2020.
- Sham Kakade and John Langford. Approximately optimal approximate reinforcement learning. In *In Proc. 19TH International Conference on Machine Learning*, pages 267–274, 2002.
- J. Kolter. The fixed points of off-policy td. In J. Shawe-Taylor, R. Zemel, P. Bartlett, F. Pereira, and K. Q. Weinberger, editors, *Advances in Neural Information Processing Systems*, volume 24. Curran Associates, Inc., 2011.
- Aviral Kumar, Justin Fu, George Tucker, and Sergey Levine. Stabilizing off-policy q-learning via bootstrapping error reduction. *CoRR*, abs/1906.00949, 2019.
- Aviral Kumar, Abhishek Gupta, and Sergey Levine. Discor: Corrective feedback in reinforcement learning via distribution correction. *CoRR*, abs/2003.07305, 2020a.
- Aviral Kumar, Aurick Zhou, George Tucker, and Sergey Levine. Conservative q-learning for offline reinforcement learning. *CoRR*, abs/2006.04779, 2020b.
- Alessandro Lazaric, Mohammad Ghavamzadeh, and Rémi Munos. Finite-sample analysis of least-squares policy iteration. *Journal of Machine Learning Research*, 13(98):3041–3074, 2012.
- Alessandro Lazaric, Mohammad Ghavamzadeh, and Rémi Munos. Analysis of classification-based policy iteration algorithms. *Journal of Machine Learning Research*, 17(19):1–30, 2016.
- Sergey Levine, Aviral Kumar, George Tucker, and Justin Fu. Offline reinforcement learning: Tutorial, review, and perspectives on open problems. *CoRR*, abs/2005.01643, 2020.
- F. Liese and I. Vajda. On divergences and informations in statistics and information theory. *IEEE Transactions on Information Theory*, 52(10):4394–4412, 2006. doi: 10.1109/TIT.2006.881731.
- T. Lillicrap, J. Hunt, A. Pritzel, N. Heess, T. Erez, Y. Tassa, D. Silver, and Daan Wierstra. Continuous control with deep reinforcement learning. *CoRR*, abs/1509.02971, 2016.
- Vincent Liu, Raksha Kumaraswamy, Lei Le, and Martha White. The utility of sparse representations for control in reinforcement learning. *CoRR*, abs/1811.06626, 2018.
- Ajay Mandlekar, Danfei Xu, Josiah Wong, Soroush Nasiriany, Chen Wang, Rohun Kulkarni, Li Fei-Fei, Silvio Savarese, Yuke Zhu, and Roberto Martín-Martín. What matters in learning from offline human demonstrations for robot manipulation. *CoRR*, abs/2108.03298, 2021.
- Volodymyr Mnih, Koray Kavukcuoglu, David Silver, Alex Graves, Ioannis Antonoglou, Daan Wierstra, and Martin Riedmiller. Playing atari with deep reinforcement learning. *Nature*, 518(7540):529–533, 2015.
- Rémi Munos. Error bounds for approximate policy iteration. In *International Conference on Machine Learning*, volume 3, pages 560–567, 2003.
- Rémi Munos. Error bounds for approximate value iteration. In *AAAI Conference on Artificial Intelligence*, pages 1006–1011, 2005.
- Rémi Munos and Csaba Szepesvári. Finite-time bounds for fitted value iteration. *Journal of Machine Learning Research*, 9(27):815–857, 2008.
- Rongjun Qin, Songyi Gao, Xingyuan Zhang, Zhen Xu, Shengkai Huang, Zewen Li, Weinan Zhang, and Yang Yu. Neorl: A near real-world benchmark for offline reinforcement learning. *CoRR*, abs/2102.00714, 2021.
- Kajetan Schweighofer, Markus Hofmarcher, Marius-Constantin Dinu, Philipp Renz, Angela Bitto-Nemling, Vihang P. Patil, and Sepp Hochreiter. Understanding the effects of dataset characteristics on offline reinforcement learning. *CoRR*, abs/2111.04714, 2021.
- David Silver, Julian Schrittwieser, Karen Simonyan, Ioannis Antonoglou, Aja Huang, Arthur Guez, Thomas Hubert, Lucas Baker, Matthew Lai, Adrian Bolton, Yutian Chen, Timothy Lillicrap, Fan Hui, Laurent Sifre, George van den Driessche, Thore Graepel, and Demis Hassabis. Mastering the game of go without human knowledge. *Nature*, 550(7676):354–359, 2017.
- Richard Sutton and Andrew Barto. *Reinforcement Learning: An Introduction*. The MIT Press, second edition, 2018.
- J.N. Tsitsiklis and B. Van Roy. An analysis of temporal-difference learning with function approximation. *IEEE Transactions on Automatic Control*, 42(5):674–690, 1997. doi: 10.1109/9.580874.
- John N. Tsitsiklis and Benjamin van Roy. Feature-based methods for large scale dynamic programming. *Machine Learning*, 22(1):59–94, Mar 1996. ISSN 1573-0565. doi: 10.1007/BF00114724.
- Hado van Hasselt, Yotam Doron, Florian Strub, Matteo Hessel, Nicolas Sonnerat, and Joseph Modayil. Deep reinforcement learning and the deadly triad. *CoRR*, abs/1812.02648, 2018.
- Ruosong Wang, Dean P. Foster, and Sham M. Kakade. What are the statistical limits of offline RL with linear function approximation? *CoRR*, abs/2010.11895, 2020.
- Christopher Watkins and Peter Dayan. Q-learning. *Machine Learning*, 8(3):279–292, 1992. ISSN 1573-0565. doi: 10.1007/BF00992698.

Tengyang Xie and Nan Jiang. Batch value-function approximation with only realizability. *CoRR*, abs/2008.04990, 2020.

Zhuoran Yang, Yuchen Xie, and Zhaoran Wang. A theoretical analysis of deep q-learning. *CoRR*, abs/1901.00137, 2019.

Shangdong Zhang, Hengshuai Yao, and Shimon Whiteson. Breaking the deadly triad with a target network. *CoRR*, abs/2101.08862, 2021.

A SUPPLEMENTARY MATERIALS FOR SECTION 2

Below, we present the pseudocode of a generic Q -learning algorithm with function approximation.

Algorithm 1 Generic Q -learning algorithm with function approximation.

```

1: initialize  $\phi_0$ 
2: initialize  $s_0 \sim p_0$ 
3: initialize  $\mathcal{D} = \emptyset$ 
4: for iteration  $k$  in  $\{K\}$  do
5:   for sampling step in  $\{S\}$  do
6:      $a_t \sim \pi_k(a_t|s_t)$  ▷ Sample from behavior policy (e.g.,  $\epsilon$ -greedy).
7:      $s_{t+1} \sim p(s_{t+1}|s_t, a_t)$ 
8:      $\mathcal{D} = \mathcal{D} \cup \{(s_t, a_t, r(s_t, a_t), s_{t+1})\}$  ▷ Append to replay memory.
9:   end for
10:   $\phi_{k,0} = \phi_k$ 
11:  for gradient step  $g$  in  $\{G\}$  do
12:    sample batch  $\{(s_t^i, a_t^i, r_t^i, s_{t+1}^i)\}$  from  $\mathcal{D}$  ▷ Sample from replay memory.
13:     $\phi_{k,g+1} \leftarrow \phi_{k,g} - \alpha \nabla_{\phi_{k,g}} \sum_i (Q_{\phi_{k,g}}(s_t^i, a_t^i) - (r_t^i + \gamma \max_{a_{t+1}} Q_{\phi_k}(s_{t+1}^i, a_{t+1}^i)))^2$ 
14:  end for
15:   $\phi_{k+1} = \phi_{k,G}$ 
16: end for

```

B SUPPLEMENTARY MATERIALS FOR SECTION 4

This section gives additional details with respect to Section 4.

B.1 SUPPLEMENTARY MATERIALS FOR SECTION 4.1

As noted in Section 4.1.1, concentrability coefficient C_3 , as defined by (1) and (3), is equivalent to an f -divergence between a given distribution β and the sampling distribution μ . As stated, that is the case when $f(x) = x^2 - 1$, since

$$\begin{aligned}
\left\| \frac{\beta}{\mu} \right\|_{2,\mu} &= \left(\mathbb{E}_{(s,a) \sim \mu} \left[\left(\frac{\beta(s,a)}{\mu(s,a)} \right)^2 \right] \right)^{1/2} \\
&= \left(\mathbb{E}_{(s,a) \sim \mu} \left[\left(\frac{\beta(s,a)}{\mu(s,a)} \right)^2 \right] - 1 + 1 \right)^{1/2} \\
&= \left(\mathbb{E}_{(s,a) \sim \mu} \left[\left(\frac{\beta(s,a)}{\mu(s,a)} \right)^2 - 1 \right] + 1 \right)^{1/2} \\
&= \left(\mathbb{E}_{(s,a) \sim \mu} \left[f \left(\frac{\beta(s,a)}{\mu(s,a)} \right) \right] + 1 \right)^{1/2} \\
&= \sqrt{\mathcal{D}_f(\beta||\mu) + 1} \\
&= \sqrt{\chi^2(\beta||\mu) + 1}.
\end{aligned}$$

As the last equality states, the f -divergence above corresponds to a particular type of divergence known as the χ^2 -divergence [Liese and Vajda, 2006].

Below, we prove Theorem 4.1. We reproduce the theorem's statement before the proof for ease of consultation.

Theorem B.1. Let $\mathcal{P}(\mathcal{S}, \mathcal{A})$ represent the set of probability distributions over $\mathcal{S} \times \mathcal{A}$. Let also $L_\mu : \mathcal{P}(\mathcal{S} \times \mathcal{A}) \rightarrow \mathbb{R}_0^+$ such

that $L_\mu(\beta) = \left\| \frac{\beta}{\mu} \right\|_{2,\mu}^2$. The solution μ to

$$\operatorname{argmin}_{\mu \in \mathcal{P}(\mathcal{S} \times \mathcal{A})} \max_{\beta \in \mathcal{P}(\mathcal{S} \times \mathcal{A})} L_\mu(\beta) \quad (5)$$

is the uniform distribution over the state-action space.

Proof. Suppose that, as discussed, the maximizing player (adversary) has access to a distribution μ , chosen by the minimizing player. The adversary's objective is therefore to maximize L_μ over the probability simplex. We begin to show what is the solution of such maximization. We start by noting that L_μ , being a norm, is a convex real function. L_μ is also continuous. Additionally, the probability simplex $\mathcal{P}(\mathcal{S} \times \mathcal{A})$ is a compact set, since it is both closed and bounded. Under the three conditions just mentioned, Bauer's Maximum Principle guarantees that the solution of the maximization lies on the subset of extreme points of the admissible region. Such set is, in the case of the probability simplex, the subset of probability distributions with a singleton support set. Equivalently, the adversary is to choose a distribution β such that, for some pair (s, a) , $\beta(s, a) = 1$ and is zero otherwise. Formally, we can write

$$L_\mu(\beta) = \sum_{(s,a) \in \mathcal{S} \times \mathcal{A}} \mu(s, a) \left(\frac{\beta(s, a)}{\mu(s, a)} \right)^2 \quad (6)$$

$$= \sum_{(s,a) \in \mathcal{S} \times \mathcal{A}} \mu(s, a)^{-1} \beta(s, a)^2. \quad (7)$$

Therefore,

$$\max_{\beta \in \mathcal{P}(\mathcal{S} \times \mathcal{A})} L_\mu(\beta) = \max_{(s,a) \in \mathcal{S} \times \mathcal{A}} \mu(s, a)^{-1}. \quad (8)$$

Finally, the minimizing player's best choice of μ is the one minimizing the quantity above. We note that

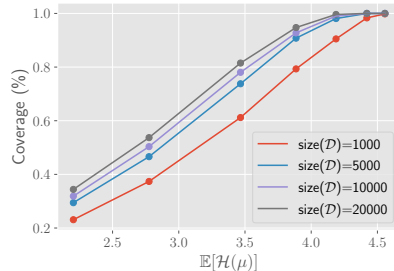
$$\max_{(s,a) \in \mathcal{S} \times \mathcal{A}} \mu(s, a)^{-1} = |\mathcal{S} \times \mathcal{A}| \quad (9)$$

if μ is the uniform distribution and

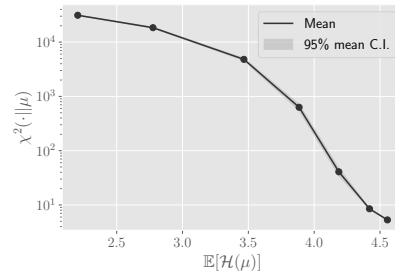
$$\max_{(s,a) \in \mathcal{S} \times \mathcal{A}} \mu(s, a)^{-1} > |\mathcal{S} \times \mathcal{A}| \quad (10)$$

otherwise. The conclusion follows. \square

Figure 8 displays the relationship between the expected entropy of the sampling distribution μ and: (i) the coverage of different datasets constructed using μ ; and (ii) the mean χ^2 -divergence to all other distributions. The plots are computed using randomly sampled distributions, which we sample from different Dirichlet distributions. We control the expected entropy of the resulting distributions by varying the Dirichlet parameter α . As seen in Fig. 8 (a), irrespectively of the dataset size, higher entropy distributions lead to datasets featuring higher coverage over the distribution support. As seen in Fig. 8 (b), higher entropy distributions yield, on average, a lower χ^2 -divergence to all other sampled distributions in comparison to lower entropy distributions.



(a) Dataset coverage.



(b) Distance to all other distributions.

Figure 8: The relationship between the expected entropy of the distribution μ and: (i) the dataset coverage; and (ii) the χ^2 -divergence to all other distributions.

B.2 SUPPLEMENTARY MATERIALS FOR SECTION 4.2

In this section we study how the data distribution can influence the performance of Q -learning based RL algorithms with function approximation, under a four-state MDP (Fig. 9). The main objective of this section is to show that the data distribution plays an active role regulating algorithmic stability. We show that the data distribution can significantly influence the quality of the resulting policies and affect the stability of the learning algorithm. We consider both online and offline RL settings. We finish this section by summarizing the key insights and providing a discussion on how the example presented here, as well as the respective findings, can generalize into bigger and more realistic MDPs.

All experimental results are averaged over 6 independent runs.

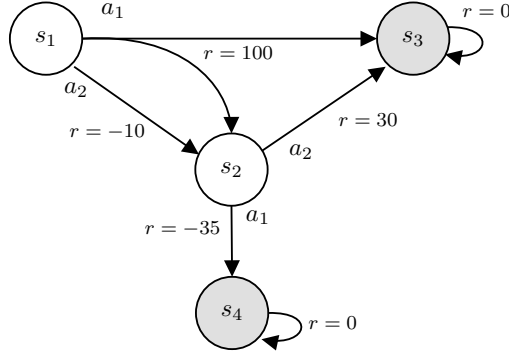


Figure 9: Four-state MDP, comprising states $\{s_1, s_2, s_3, s_4\}$ and actions $\{a_1, a_2\}$. State s_1 is the initial state and states s_3 and s_4 are the terminal absorbing states. All actions lead to deterministic transitions, except for the state-action pair (s_1, a_1) , where $p(s_3|s_1, a_1) = 0.99$ and $p(s_2|s_1, a_1) = 0.01$. The reward function is defined as $r(s_1, a_1) = 100$, $r(s_1, a_2) = -10$, $r(s_2, a_1) = -35$ and $r(s_2, a_2) = 30$.

We focus our attention on non-terminal states s_1 and s_2 of the MDP, whose optimal Q -function is

$$Q^* = \begin{matrix} & a_1 & a_2 \\ \begin{matrix} s_1 \\ s_2 \end{matrix} & \begin{bmatrix} 100.3 & 20 \\ -35 & 30 \end{bmatrix} \end{matrix}.$$

At state s_1 the correct action is a_1 , whereas at state s_2 the correct action is a_2 . We set $\gamma = 1$.

We consider a linear function approximator $Q_w(s_t, a_t) = w^T \phi(s_t, a_t)$, where $w = [w_1, w_2, w_3]^T$ denotes a weight column vector and ϕ is a feature mapping, defined as $\phi(s_1, a_1) = [1, 0, 0]^T$, $\phi(s_1, a_2) = [0, 1, 0]^T$, $\phi(s_2, a_1) = [\alpha, 0, 0]^T$, and $\phi(s_2, a_2) = [0, 0, 1]^T$

$$Q_w = \begin{matrix} & a_1 & a_2 \\ \begin{matrix} s_1 \\ s_2 \end{matrix} & \begin{bmatrix} w_1 & w_2 \\ \alpha w_1 & w_3 \end{bmatrix} \end{matrix},$$

where $\alpha \in [1, 3/2)$. The optimal policy is retrieved if $w_1 > w_2$ and $\alpha w_1 < w_3$. As can be seen, due to the choice of feature mapping, the capacity of the function approximator is limited and there exists a correlation in the features between $Q_w(s_1, a_1)$ and $Q_w(s_2, a_1)$. This will be key to the results that follow.

B.2.1 Offline Oracle Version

We start by assuming that we have access to an oracle providing us with the exact optimal Q -function and write the loss of the function approximator as

$$\mathcal{L}(w) = \mathbb{E}_{(s_t, a_t) \sim \mu} \left[\left(w^T \phi(s_t, a_t) - Q^*(s_t, a_t) \right)^2 \right],$$

where μ can be interpreted as the probability distribution over state-action pairs induced by a static dataset of transitions or a generative model of the environment. The optimal weight vector is given by

$$w_1^* = \frac{\mu(s_1, a_1)Q^*(s_1, a_1) + \alpha\mu(s_2, a_1)Q^*(s_2, a_1)}{\mu(s_1, a_1) + \alpha^2\mu(s_2, a_1)}, \quad w_2^* = Q^*(s_1, a_2), \quad w_3^* = Q^*(s_2, a_2), \quad (11)$$

as long as $\mu(s, a) > 0, \forall (s, a)$. In the results that follow, we focus our attention on the proportion between probabilities $\mu(s_2, a_1)$ and $\mu(s_1, a_1)$, thus setting $\mu(s_2, a_1) = 1 - \mu(s_1, a_1)$. Figure 10 (a) displays the influence of the data distribution, namely the proportion between $\mu(s_1, a_1)$ and $\mu(s_2, a_1)$, on the learned policy when $\alpha = 5/4$. As can be seen, for the present MDP, the optimal policy is only attained if $\mu(s_1, a_1) \approx 0.5$ and $\mu(s_2, a_1) \approx 0.5$. Precisely, as aforementioned, the optimal policy is retrieved if $w_1^* > w_2^*$ and $\alpha w_1^* < w_3^*$. Such inequalities are verified when

$$\frac{\alpha(20\alpha + 35)}{80.3 + 35\alpha + 20\alpha^2} < \mu(s_1, a_1) < \frac{65\alpha^2}{65\alpha^2 + 100.3\alpha - 30}$$

$$(\approx 0.48) < \mu(s_1, a_1) < (\approx 0.51).$$

However, as can be seen in the figure, if $\mu(s_1, a_1)$ is not ≈ 0.5 , the optimal policy will not be retrieved. As an example, if $\mu(s_1, a_1) = 0.7$ and $\mu(s_1, a_2) = 0.3$, we have $w_1^* \approx 48.8$, $w_2^* = 20$ and $w_3^* = 30$. Thus, the policy is correct at state s_1 since $w_1^* > w_2^*$, but wrong at state s_2 since condition $\alpha w_1^* < w_3^*$ is not verified. We observe a somewhat similar trend for $\alpha \in [1, 3/2)$, as can be seen in Figure 10 (b): the retrieval of the optimal policy is dependent on $\mu(s_1, a_1)$ and $\mu(s_2, a_1)$.

The results above show that, due to the limited approximation power and correlation between features, the data distribution impacts the performance of the resulting policies, even for the presently considered oracle-based algorithm (with access to the true Q^* function). The number of retrieved correct actions is directly dependent on the properties of the data distribution.

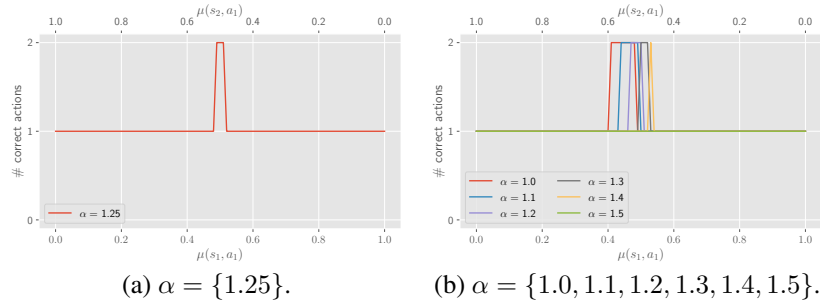


Figure 10: The number of correct actions at states s_1 and s_2 of the four-state MDP for different data distributions. The number of correct actions is calculated using Eqs. 11 for different $\mu(s_1, a_1)$ and $\mu(s_1, a_2)$ proportions.

B.2.2 Offline Temporal Difference Version

Naturally, practical algorithms do not have access to the unknown target, Q^* . A common choice of replacement is to use the one-step temporal difference target. In such cases, the loss function becomes

$$\mathcal{L}(w) = \mathbb{E}_{(s_t, a_t, s_{t+1}) \sim \mu} \left[\left(r(s_t, a_t) + \max_{a_{t+1} \in \mathcal{A}} w^\top \phi(s_{t+1}, a_{t+1}) - w^\top \phi(s_t, a_t) \right)^2 \right].$$

If we neglect the influence of the weight vector in the target (semi-gradient), the update equation for the weight vector is given by

$$w_{t+1} = w_t - \eta \frac{\partial \mathcal{L}(w)}{\partial w}$$

$$= w_t + \eta \mathbb{E}_{(s_t, a_t, s_{t+1}) \sim \mu} \left[\left(r(s_t, a_t) + \max_{a_{t+1} \in \mathcal{A}} w_t^\top \phi(s_{t+1}, a_{t+1}) - w_t^\top \phi(s_t, a_t) \right) \phi(s_t, a_t) \right].$$

where η denotes the learning rate. Component-wisely,

$$\begin{aligned}
w_{1,t+1} &= w_{1,t} + \eta \mu(s_1, a_1) (r(s_1, a_1) + p(s_2|a_1, a_1) \max\{Q_w(s_2, a_1), Q_w(s_2, a_2)\} - w_{1,t}) \\
&\quad + \eta \mu(s_2, a_1) (r(s_2, a_1) - \alpha w_{1,t}) \alpha \\
&= w_{1,t} + \eta \mu(s_1, a_1) (r(s_1, a_1) + p(s_2|a_1, a_1) \max\{\alpha w_{1,t}, w_{3,t}\} - w_{1,t}) \\
&\quad + \eta \mu(s_2, a_1) (r(s_2, a_1) - \alpha w_{1,t}) \alpha, \\
w_{2,t+1} &= w_{2,t} + \eta \mu(s_1, a_2) (r(s_1, a_2) + \max\{Q_w(s_2, a_1), Q_w(s_2, a_2)\} - w_{2,t}) \\
&\quad \propto w_{2,t} + \eta (r(s_1, a_2) + \max\{\alpha w_{1,t}, w_{3,t}\} - w_{2,t}), \\
w_{3,t+1} &= w_{3,t} + \eta \mu(s_2, a_2) (r(s_2, a_2) - w_{3,t}) \\
&\quad \propto w_{3,t} + \eta (r(s_2, a_2) - w_{3,t}).
\end{aligned} \tag{12}$$

Figure 11 (a) displays the influence of the data distribution, namely the proportion between $\mu(s_1, a_1)$ and $\mu(s_2, a_1)$, on the retrieved policy. As can be seen, we identify three regimes: (i) whenever $\mu(s_1, a_1) \approx 0.5$, we retrieve the optimal policy (i.e., the actions are correct at both states s_1 and s_2); (ii) if $\mu(s_1, a_1) < (\approx 0.48)$ or $(\approx 0.52) < \mu(s_1, a_1) < (\approx 0.65)$, the policy is only correct at one of the states; (iii) if $\mu(s_1, a_1) > (\approx 0.65)$, the policy is wrong at both states.

Akin to the oracle version (Eqs. 11), the data distribution plays a key role in the performance of the resulting policies. However, for the present temporal difference target, the impact of the data distribution is enhanced due to the dependence of the target on the weight vector. As an example, if $\mu(s_1, a_1) = 0.7$ and $\mu(s_1, a_2) = 0.3$, we have $w_1^* \approx 49.0$, $w_2^* \approx 51.3$ and $w_3^* = 30$. As $\mu(s_1, a_1)$ increases, not only w_1 increases (similarly to the oracle version), but also w_2 wrongly increases. This is due to the fact that the target used in the estimation of w_2 depends on w_1 (Eqs. 12).

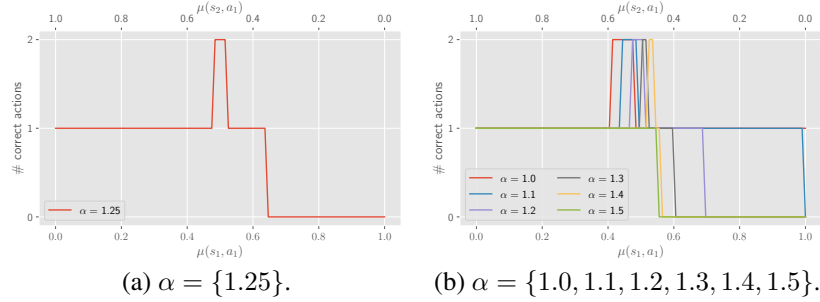


Figure 11: The number of correct actions at states s_1 and s_2 of the four-state MDP for different data distributions. The number of correct actions is calculated by finding the fixed-point of Eqs. 12 for different $\mu(s_1, a_1)$ and $\mu(s_1, a_2)$ proportions.

B.2.3 Online Temporal Difference Version with Unlimited Replay Capacity

Reinforcement learning algorithms usually collect data in an online fashion, by using an exploratory policy such as an ϵ -greedy policy with respect to the current Q -values estimates. We now focus on such setting, showing that similar problems arise for the previously presented MDP and set of features. Instead of considering a fixed μ distribution, we now consider a setting where the μ distribution is dynamically induced by a replay buffer. We focus our attention on the commonly used ϵ -greedy exploration.

Figures 12 and 13 display the experimental results for the four-state MDP when $\alpha = 1.2$, under two different exploratory policies: (i) a fully exploratory policy, i.e., an ϵ -greedy policy with $\epsilon = 1.0$; and (ii) an ϵ -greedy policy with $\epsilon = 0.05$. Under the current experimental setting, we consider a replay buffer size big enough such that we never discard old transitions. We use an uniform synthetic data distribution, i.e., $\mu(s_1, a_1) = \mu(s_1, a_2) = \mu(s_2, a_1) = \mu(s_2, a_2) = 0.25$, as baseline.

With respect to the uniform baseline, as can be seen in Fig. 12, it outperforms all other data distributions, yielding two correct actions, higher reward, and lower Q -values error. This is expected, as previously discussed, since under this synthetic distribution we have that $\mu(s_1, a_1) = \mu(s_2, a_1)$.

Regarding the fully exploratory policy, i.e., the ϵ -greedy policy with $\epsilon = 1.0$, the agent is only able to pick the correct action at state s_1 , featuring a lower reward and higher average Q -value error in comparison to the uniform distribution

baseline. This is due to the fact that the stationary distribution of the MDP under the fully exploratory policy is too far from the uniform distribution to retrieve the optimal policy. As seen in Fig. 13 (b), under the stationary distribution, we have $\mu(s_1, a_1) \approx 0.1$ and $\mu(s_2, a_1) \approx 0.05$. If we normalize the μ distribution accounting only for $\mu(s_1, a_1)$ and $\mu(s_2, a_1)$ probabilities we have that $\mu(s_1, a_1) \approx 0.7$ and $\mu(s_2, a_1) \approx 0.3$. As seen in Fig. 11, under such proportion of $\mu(s_1, a_1)$ and $\mu(s_2, a_1)$ probabilities, we only yield one correct action, as verified by the experiment.

Finally, for the ϵ -greedy policy with $\epsilon = 0.05$, the performance of the agent further deteriorates, as displayed in Fig. 12. As can be seen in Fig. 12 (c) and Fig. 14, such exploratory policy induces oscillations in the Q -values, which eventually damp out as learning progresses. The oscillations arise due to an undesirable interplay between the features of the function approximator and the data distribution: exploitation leads to changes in distribution μ that, in turn, drive changes in the weight vector w (which implicitly regulates the action selection mechanism). The oscillations end up being dampened by the fact that the replay buffer contributes to stabilize the data distribution in such a way that exploitation will not lead to such big changes in the μ distribution. As μ approaches its stationary distribution (since the replay buffer is sufficiently large), we have that $Q_w(s_1, a_1) \approx Q_w(s_1, a_2)$ and $Q_w(s_2, a_1) > Q_w(s_2, a_2)$, as can be seen in Fig. 14 (b). We reach an undesirable solution: the agent cannot distinguish which is the best action at state s_1 . Thus, it keeps alternating between actions a_1 and a_2 at state s_1 , as seen in Fig. 12 (a).

Detailed description of the interplay between the features of the function approximator and the data distribution under the ϵ -greedy exploratory policy with $\epsilon = 0.05$: (i) in early episodes, exploitation leads to an increase in the probability of sampling state-action pair (s_1, a_1) from the replay buffer since we estimate that $Q_w(s_1, a_1) > Q_w(s_1, a_2)$ (Fig. 14 (b)). This is clearly seen in Fig. 13 (c), as $\mu(s_1, a_1)$ features a steep increase in probability during early training; (ii) the increase in probability $\mu(s_1, a_1)$, as well as decrease in probability $\mu(s_2, a_1)$, drives an increase in weight w_1 , as previously discussed; (iii) due to the fact that the target used in the estimation of w_2 , associated with $Q_w(s_1, a_2)$, depends on w_1 (Eqs. 12), the increase in w_1 will also drive an increase in w_2 . However, the increase in weight w_2 is slower than the increase in weight w_1 because the pair (s_1, a_2) is underrepresented in the replay buffer, i.e., the learning of $Q_w(s_1, a_2)$ occurs at a much slower pace than that of $Q_w(s_1, a_1)$. Nevertheless, happens that, when a certain threshold is surpassed, we wrongly estimate $Q_w(s_1, a_1) < Q_w(s_1, a_2)$, as can be seen in Fig. 14 (b) around episode 2 500. This leads to a drop in the obtained reward and number of correct actions, as seen in Fig. 12, due to the fact that action a_2 is wrongly taken at state s_1 ; (iv) since we now wrongly estimate $Q_w(s_1, a_1) < Q_w(s_1, a_2)$, exploitation leads to an increase in probabilities $\mu(s_1, a_2)$ and $\mu(s_2, a_1)$, driving weight w_1 down, until $\mu(s_1, a_1)$ is low enough such that we correctly estimate $Q_w(s_1, a_1) > Q_w(s_1, a_2)$ again. As can be seen in Fig. 13 (c), after an initial increase, we observe a decrease in probability $\mu(s_1, a_1)$, as well as increase in probability $\mu(s_2, a_1)$, between episodes 2500 and 5000; The increase in probability $\mu(s_2, a_1)$ is driven by the fact that $Q_w(s_2, a_1) > Q_w(s_2, a_2)$ always verifies (Fig. 14 (b)); (v) the described interplay repeats again. However, the oscillation is now dampened by the fact that the replay buffer is already partially-filled with previous experience.



Figure 12: Four-state MDP experiments for different exploratory policies with an infinitely-sized replay buffer.

B.2.4 Online Temporal Difference Version with Limited Replay Capacity

Lastly, we consider an experimental setting where the replay buffer has limited capacity. Figures 15 and 16 display the experimental results obtained with the ϵ -greedy exploratory policy with $\epsilon = 0.05$ by varying the size/capacity of the replay buffer. As can be seen in Fig. 16, as the replay buffer size increases, the amplitude of the oscillations in the μ distribution gets smaller. Moreover, as the replay buffer size increases, the oscillations in the Q -values and Q -values errors are smaller, as seen in Fig. 15. Given the previous discussion, the obtained results are expected. The undesirable interplay between the function approximator and the data distribution repeats as previously discussed for the infinitely-sized replay buffer.

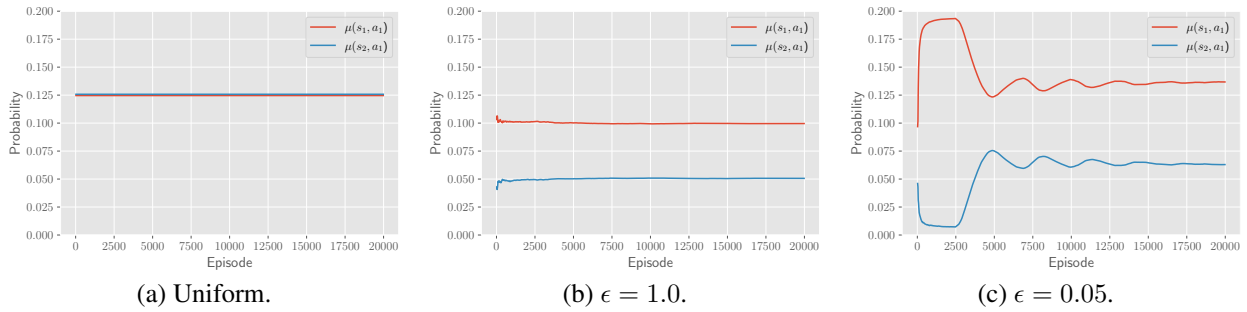


Figure 13: Four-state MDP experiments for different exploratory policies with an infinitely-sized replay buffer. The plots display the data distribution probabilities $\mu(s_1, a_1)$ and $\mu(s_2, a_1)$, as induced by the contents of the replay buffer, throughout episodes.

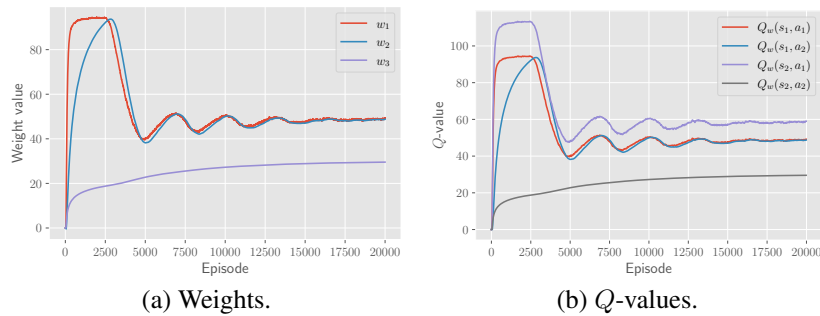


Figure 14: Four-state MDP experiments for the ϵ -greedy exploratory policy with $\epsilon = 0.05$ and an infinitely-sized replay buffer. The plots display the estimated weights and Q -values throughout episodes.

However, as the replay buffer gets smaller, the more the data distribution induced by the contents of the replay buffer is affected by changes to the current exploratory policy, in this case the ϵ -greedy exploratory policy. Therefore, for smaller replay buffers, exploitation leads to more steep changes in $\mu(s_1, a_1)$ and $\mu(s_2, a_1)$ probabilities, as seen in Fig. 16 (a). Such changes in the μ distribution drive abrupt changes in weights w_1 and w_2 , as well as estimated Q -values, as seen in Fig. 15 (a). Similarly to the infinitely-sized replay buffer, the agent keeps alternating between phases where it estimates that $Q_w(s_1, a_1) > Q_w(s_1, a_2)$ and phases where it estimates the opposite. However, the period at which phases switch is rather longer for smaller replay buffer sizes. Whereas for the infinitely-sized replay buffer the amplitude of the oscillations is dampened due to the fact that previously stored experience contributes to make the data distribution more stationary, this is not as easily achieved by smaller replay buffers. As our results suggest, the size of the replay buffer influences the stability of the data distribution, which can, in turn, affect the stability of the learning algorithm and quality of the resulting policies.

B.2.5 Discussion

In summary, this manuscript presented a set of experiments under a four-state MDP that show how the data distribution can greatly influence the performance of the resulting policies and the stability of the learning algorithm. First, we showed that, under offline RL settings, the number of correct actions is directly dependent on the properties of the data distribution due to an undesirable correlation between features. Second, under online RL settings, not only the quality of the retrieved policies depends on the data collection mechanism, but also an undesirable interplay between the data distribution and the function approximator can arise: exploitation can lead to abrupt changes in the data distribution, thus hindering learning. Additionally, we showed that the replay buffer size can also affect the learning stability.

Above all, the results presented emphasize the key role played by the data distribution in the context of off-policy RL algorithms with function approximation. Despite the fact that we study a four-state MDP, we argue that the example here presented can generalize into more realistic settings. In the first place, it is possible to construct an MDP such that the learning dynamics under a function approximator with state-dependent features are equivalent to the previously discussed

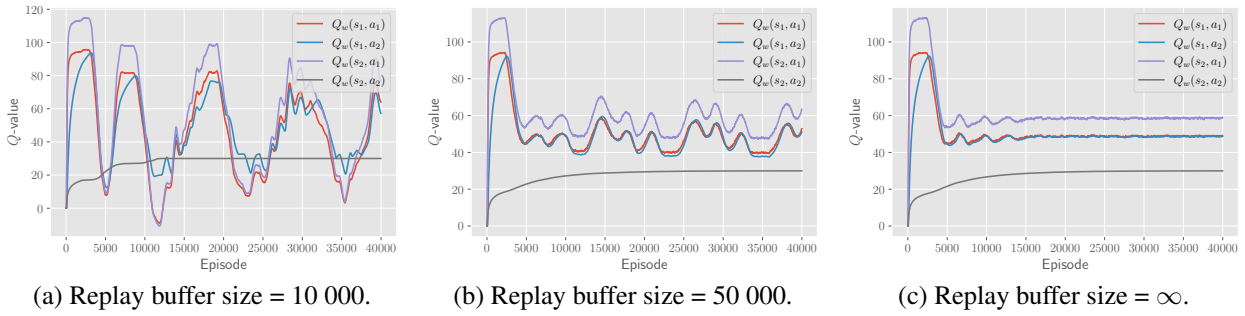


Figure 15: Four-state MDP experiments for the ϵ -greedy exploratory policy with $\epsilon = 0.05$ under different replay buffer sizes. The plots display the estimated Q -values throughout episodes.

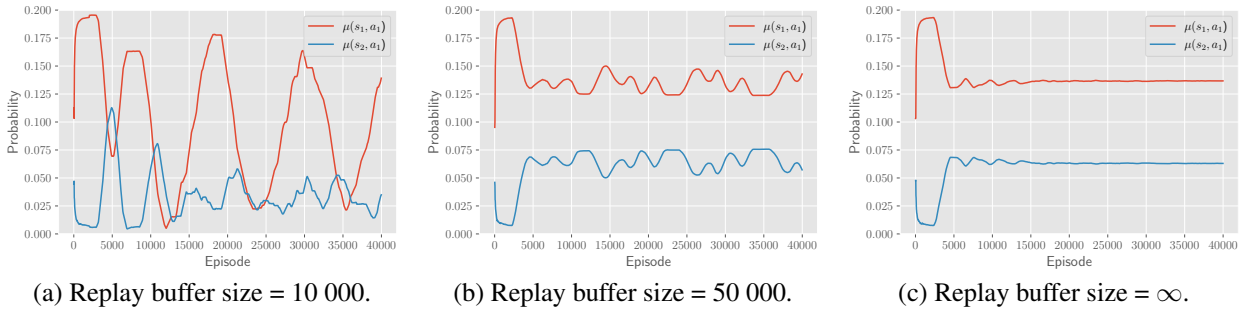


Figure 16: Four-state MDP experiments for the ϵ -greedy exploratory policy with $\epsilon = 0.05$ under different replay buffer sizes. The plots display the data distribution probabilities $\mu(s_1, a_1)$ and $\mu(s_2, a_1)$, as induced by the contents of the replay buffer, throughout episodes.

approximator with (state, action)-dependent features. Second, we can abstract the example here presented by hypothesizing that states s_1 and s_3 can correspond to states along an optimal trajectory of a larger MDP, and state s_2 to a state outside the optimal trajectory. If the features of the states are wrongly correlated (as in the example, we have a correlation between the features of states s_1 and s_2), exploitation along the optimal trajectory can deteriorate the Q -values for states outside the optimal trajectory (as in the example, state s_3), which can give rise to algorithmic instabilities.

C SUPPLEMENTARY MATERIALS FOR SECTION 5

This section gives additional details with respect to Section 5. The section is divided as follows:

- subsection C.1: Experimental environments.
- subsection C.2: Experimental methodology.
- subsection C.3: Implementation details and algorithms hyperparameters.
- subsection C.4: Complete experimental results.

C.1 EXPERIMENTAL ENVIRONMENTS

Below, we detail the experimental environments used in this work.

C.1.1 Grid 1 and Grid 2 Environments

The grid 1 environment comprises a tabular 8×8 grid, as seen in Fig. 17 (a). The agent starts in the lower left corner ('S' square) and aims to reach the upper right corner ('G' square) as fast as possible. The grid 2 environment, as seen in Fig. 17

(b), comprises a tabular 8×8 grid, with walls in the middle of the environment. The agent starts in the lower left square ('S' square) and aims to reach the upper right square ('G' square) as fast as possible.

Common to both environments, the episodes have a fixed length of 50 timesteps. The action set is {up, down, right, left, stay}. No diagonal movements are allowed. All actions lead to deterministic state transitions except for against-wall actions (the environments are virtually delimited by four walls); in such cases the agent has a 0.01 probability of moving to an adjacent square and with the remainder probability stays at the same square. The reward at each timestep is one if the agent is at the goal state and zero otherwise. The underlying MDPs comprise $(8 \times 8) \times 5 = 320$ state-action pairs.

Regarding the state features, each state is mapped to a 8-dimensional vector. Each entry of the vector is drawn, independently, from a uniform distribution in $[-1, 1]$. The state features are pre-computed during initialization and kept constant throughout training. We set the discount factor γ to 0.9.

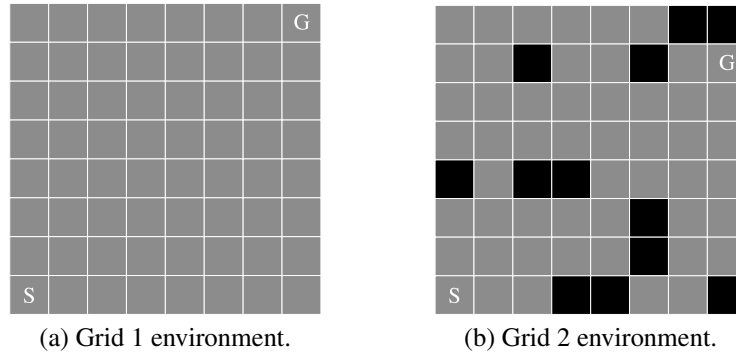


Figure 17: Illustration of the grid environments.

C.1.2 Multi-path Environment

The multi-path environment (k, l) , displayed in Fig. 18, comprises k parallel paths of length l . The agent starts in the left-most state and aims to reach one of the k absorbing states with positive reward on the right, while avoiding to fall into the absorbing state with zero reward. In other words, the agent aims at following one of the k paths all the way until the positive-rewarding state without falling into the absorbing zero reward state.

The action set is $\{1, 2, 3, \dots, k\}$. All actions lead to deterministic state transitions except for the action taken in the initial state; at the initial state, the agent's action succeeds with probability $1 - p$ and with probability p , the agent will randomly enter the first state of one of the k paths. By default we set $p = 0.01$. The reward is one if the agent is at one of the k final absorbing states of the path and zero everywhere else. The episode length is 10 timesteps. By default, we set $k = 5$ and $l = 5$. Therefore, the underlying MDP comprises $(k \times l + 2) \times k = 135$ state-action pairs.

Regarding the state features, each state is mapped to a 4-dimensional vector. Each entry of the vector is drawn from a uniform distribution in $[-1, 1]$. The state features are pre-computed during initialization and kept constant throughout training. We set the discount factor γ to 0.9.

C.1.3 Pendulum, Cartpole and Mountaincar Environments

The pendulum, cartpole and mountaincar environments are based on the OpenAI gym environments implementations. For all environments, we set the discount factor γ to 0.99. For the pendulum environment, the action space is discretized into 5 equally-spaced discrete actions.

For all environment, and only with the purpose of calculating different properties of the datasets (such as coverage, or entropy), we discretized the state-space. We used an histogram-like discretization with equally spaced bins. For both the pendulum and mountaincar environments we discretized each dimension of the state-space using 50 bins; for the cartpole environment we used 20 bins per state-space dimension.

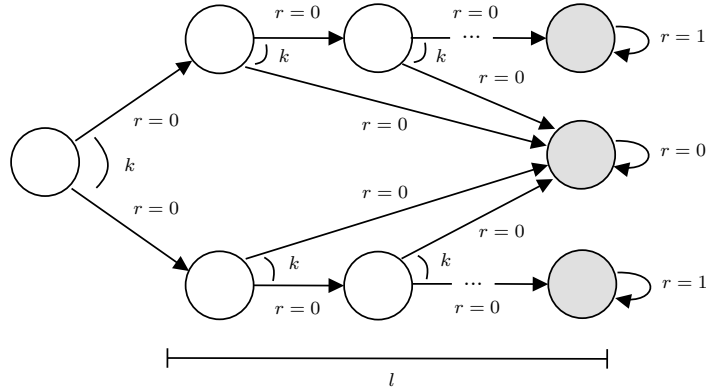


Figure 18: Illustration of the multi-path (k, l) environment.

C.2 EXPERIMENTAL METHODOLOGY

In order to reliably compare the different algorithms used in this work, we followed a rigorous experimental evaluation methodology. Under each experimental configuration, we perform 4 training runs. Each training run is punctually evaluated during training, as well as at the end of training, by running 5 evaluation rollouts. Each rollout comprises a full-length episode. We then average the resulting (4×5) performance indicators per train run, thus obtaining 4 performance samples. We focus our attention on two main types of performance indicators: (i) the reward obtained under evaluation rollouts; and (ii) the Q -values errors, calculated using a value-iteration or Q -learning solution for the same MDP;

C.3 IMPLEMENTATION DETAILS AND HYPERPARAMETERS

We developed our software in a Python environment, using the following additional open-source frameworks: ACME [Hoffman et al., 2020], and Tensorflow [Abadi et al., 2015]. Table 1 presents the default hyperparameters for the offline DQN and CQL algorithms used in the experiments presented in Section 5.

Table 1: Algorithms hyperparameters used under Section 5 experiments.

Hyperparameter	Value(s)	Hyperparameter	Value(s)	Hyperparameter	Value(s)
Optimizer	Adam	Optimizer	Adam	Optimizer	Adam
Learning rate	1e-3	Learning rate	1e-3	Learning rate	1e-3
Discount factor (γ)	0.9	Discount factor (γ)	0.99	Discount factor (γ)	0.99
Dataset size	50 000	Dataset size	200 000	Dataset size	1 000 000
Batch size	100	Batch size	100	Batch size	100
Target update period	1 000	Target update period	1 000	Target update period	1 000
Num. learning steps	100 000	Num. learning steps	200 000	Num. learning steps	500 000
Network layers	[20,40,20]	Network layers	[64,128,64]	Network layers	[64,128,64]
Alpha (CQL param.)	1.0	Alpha (CQL param.)	1.0	Alpha (CQL param.)	1.0

(a) Grid 1, 2 and multi-path envs.

(b) Pendulum and mountaincar envs.

(c) Cartpole env.

C.4 COMPLETE EXPERIMENTAL RESULTS

The complete experimental results can be found in the following interactive dashboard: <https://rl-data-distribution.herokuapp.com/>.